

Rapid calculations for boundary-layer transfer using wedge solutions and asymptotic expansions

By H. J. MERK

Koninklijke/Shell-Laboratorium, Amsterdam, Holland

(Received 28 July 1958)

Exact transfer calculations for boundary layers with longitudinal pressure gradients are very complicated, but in the literature several approximate methods are known for the rapid calculation of both the wall friction and the heat transfer. A 'wedge method' propounded by Meksyn turns out to be one of the most rapid methods, being no less accurate than other approximate methods. A way of refining this method is proposed.

This paper also shows that asymptotic expansions provide convenient relations which are capable of expressing the Nusselt number explicitly in terms of the Prandtl number.

It is shown that, together with the asymptotic expansions, Meksyn's method permits rapid calculation of local heat transfer numbers. Some examples of application are given for elliptical cylinders and spheres for several values of the Prandtl number.

1. Introduction

This paper is concerned with the transfer of heat and mass from a body placed in a stream. Provided the Reynolds number of the flow lies within the approximate range from 10^2 to 10^5 , we may state:

Assumption I. The transfer phenomena in the vicinity of a body submerged in a streaming fluid may be described by the laminar boundary-layer theory.

Furthermore we introduce:

Assumption II. There are no external volume forces in the streaming fluid.

This excludes free convection, so that we are only concerned with forced convection phenomena. Thus we include:

Assumption III. The main flow outside the boundary layer is irrotational.

This means that the intensity of the turbulence in the main flow has to be very low and that this flow may be calculated by means of the potential theory.

Restricting ourselves to the calculation of friction and heat transfer in unitary systems, we are only concerned with two boundary layers, viz. the dynamic boundary layer in which the transfer of momentum occurs, and the thermal boundary layer in which the transfer of heat occurs. It is well known that the boundary-layer theory can only be applied if the thickness δ of the dynamic boundary layer is small enough. If this condition is satisfied, we may ask whether or not the thickness δ_T of the thermal boundary layer is small enough to permit the application of the boundary-layer approximations to the calculation of the heat transfer.

It is known that $\delta_T < \delta$ for $\chi < \nu$, χ being the thermal diffusivity of the fluid and ν its kinematic viscosity. Introducing the Prandtl number $\sigma = \nu/\chi$, we conclude that for $\sigma > 1$, when δ is small enough, δ_T is small *a fortiori*. Hence, assumption I is legitimate if the thickness of the dynamic boundary layer is small enough.

For $\sigma < 1$, the thickness of the thermal boundary layer is greater than that of the dynamic boundary layer, so that in this range of the Prandtl number it may not suffice to assume that the thickness of the dynamic boundary layer is small enough. The limit $\sigma \rightarrow 0$ must especially be considered with care. This limit may be relevant if the kinematic viscosity is small (but finite) and the thermal diffusivity is very large. In this case the boundary-layer concept is not applicable to the calculation of the heat transfer, although it is applicable to the calculation of the friction. On the other hand, it is possible that at the limit $\sigma \rightarrow 0$ the kinematic viscosity approaches zero at small (but finite) values of the thermal diffusivity. This means that for $\sigma = 0$ we are concerned with heat transfer in a thermal boundary layer in a potential flow around the body considered. This problem has been investigated with great elegance by Boussinesq (1903, 1905) (see also Drew 1931), who introduced the concept of the thermal boundary layer before Prandtl (1904) proposed an analogous concept for the transfer of momentum. As a corollary of assumption I, we have thus to conclude that for $\sigma \rightarrow 0$ the boundary-layer theory of the heat transfer changes into Boussinesq's theory.

Although the boundary-layer concept simplifies the calculations considerably, the solution of the boundary-layer equations is generally still troublesome. The exact solution for boundary layers with an arbitrary longitudinal pressure gradient consists essentially in constructing power series in terms of the distance from the forward stagnation point of the body. The exact calculations by means of series expansion are cumbersome, because the convergence of the series is mostly bad. It is, therefore, generally necessary to perform the exact calculations numerically if the distance from the forward stagnation point is too large for the series expansion to be applied (e.g. see Prandtl 1938; Görtler 1939; Frössling 1940). In order to avoid the lengthy exact calculations, several approximate methods have been developed.

One of the best-known approximate methods is that of von Kármán (1921) and K. Pohlhausen (1921). Generally, this method is still troublesome and its accuracy is disappointing. Hence, we shall consider another group of approximate methods, called here the 'wedge methods', because these methods are based upon the well-known solutions of the boundary-layer equations for wedge-shaped profiles. The first wedge method was propounded by Falkner & Skan (1930, 1931). This method has been modified by Eckert (1942), Schuh (1949, 1954), Eckert & Livingood (1953), Kotschin & Loizjanski (see Kotschin, Kibel & Rose 1955), and by Smith (1956). All these wedge methods bear the same characteristic features: they are rapid and based upon some arbitrary hypothesis of physical nature, which has to be introduced in order to find the wedge element 'equivalent' to the element of the profile considered. The wedge methods of the authors named above differ only in the hypothesis used. Their fundamental disadvantage is that it is not clear how the calculations are to be improved if more accurate results are desired.

Meksyn (1947, 1948) has developed a method of calculation for the dynamic boundary layer, which may also be considered as a wedge method. This method consists essentially of a transformation of the boundary-layer equations and a mathematical simplification of the transformed equations. A great advantage of Meksyn's method is that no physical hypothesis is needed; the simplifications introduced are of a mathematical nature. As a result, it is possible to refine the calculations in a straightforward way. Furthermore, Meksyn's method has the following three advantages: (1) For wedge-shaped profiles (and hence in the vicinity of the forward stagnation point) the method yields exact results. (2) It may be expected that for arbitrary profiles successive refinements of the method converge towards the exact solution. (3) The method provides probably one of the most rapid calculations hitherto propounded in the literature.

It is quite easy to extend Meksyn's method to the calculation of heat transfer. In his original papers Meksyn applied complicated transformations allowing for the extension of the equations to lower values of the Reynolds number. If we are concerned with the pure boundary-layer equations only, it is possible to obtain Meksyn's final equations in a simple way. This will be shown in the next section.

In the present paper we have restricted ourselves to the most simple boundary-layer problems by the introduction of the following two assumptions:

Assumption IV. All physical quantities (viscosity, thermal conductivity, heat capacity) of the fluid are constant throughout the boundary layer.

Assumption V. The Mach number of the flow is low. The latter assumption means that in the thermal energy equations the dissipation and pressure terms may be neglected, while furthermore the density of the fluid may be considered as a constant.

It has to be stressed that the last two assumptions are not essential for the application of Meksyn's method.

2. Fundamental equations

Let us consider steady two-dimensional or rotationally symmetrical boundary-layer flows. For these cases we may introduce the coordinates (x, y) , x being the distance from the forward stagnation point measured along the circumference of the two-dimensional profile or median line of the rotationally symmetrical body, and y being the normal distance from the wall of the body. For rotationally symmetrical bodies we also introduce r , the distance from a surface element of the body to the axis of symmetry. Denoting the components of the velocity parallel to the x - and y -axis by u and v respectively and making use of assumption IV, the equations of the dynamic boundary layer are

$$\left(u \frac{\partial}{\partial x} + v \frac{\partial}{\partial y}\right) u = -\frac{1}{\rho} \frac{\partial p}{\partial x} + \nu \frac{\partial^2 u}{\partial y^2}, \quad (1)$$

$$\frac{\partial p}{\partial y} = O(1), \quad (2)$$

$$\frac{\partial(ru)}{\partial x} + \frac{\partial(rv)}{\partial y} = 0. \quad (3)$$

(Note that equation (2) holds for curved surfaces; for flat surfaces we may put $\partial p/\partial y = 0$.) These are the boundary-layer equations for rotationally symmetrical bodies. For a two-dimensional boundary layer, equations (1) and (2) retain the same forms, but in the continuity equation (3) r has to be dropped. Hence, the two-dimensional boundary-layer equations are formally obtained from (1), (2) and (3) by putting r equal to a constant. From (1) and the well-known fact that at the end of the boundary layer $\partial u/\partial y$ and $\partial^2 u/\partial y^2$ are very small, we obtain

$$\frac{\partial p}{\partial x} \doteq \frac{dp_e}{dx} = -\rho u_e \frac{du_e}{dx}, \tag{4}$$

where subscript e denotes the conditions at the end of the boundary layer. The boundary conditions are

$$u = v = 0 \text{ for } y = 0, \quad \text{and} \quad u \rightarrow u_e \text{ for } y \rightarrow \infty. \tag{5}$$

For the calculation of the heat transfer, we also need the thermal energy equation. Denoting the temperature by T and making use of the assumptions IV and V, the boundary-layer approximation to the thermal energy equation becomes

$$\left(u \frac{\partial}{\partial x} + v \frac{\partial}{\partial y}\right) T = \chi \frac{\partial^2 T}{\partial y^2}, \tag{6}$$

with the boundary conditions

$$T = T_w \text{ for } y = 0, \quad \text{and} \quad T \rightarrow T_e \text{ for } y \rightarrow \infty, \tag{7}$$

where the subscript w denotes the conditions at the wall.

In order to satisfy (3), a stream function ψ is introduced, such that

$$u = \frac{L}{r} \frac{\partial \psi}{\partial y}, \quad v = -\frac{L}{r} \frac{\partial \psi}{\partial x}, \tag{8}$$

L being a reference length of the body considered. For $r = L$, (8) defines the stream function of a two-dimensional flow.

The x and y coordinates will now be transformed by writing

$$\xi = \int_0^x \frac{u_e(x) r^2 dx}{V L^2 L}, \quad \eta = \left(\frac{R}{2\xi}\right)^{\frac{1}{2}} \frac{u_e r y}{V L L}, \tag{9}$$

where V is the velocity of the oncoming flow, and $R = VL/\nu$. The stream function $\psi(x, y)$ will be written

$$\psi(x, y) = VL(2\xi/R)^{\frac{1}{2}} f(\xi, \eta). \tag{10}$$

Equations (9) and (10) represent the essential parts of Meksyn's transformations; and it is easily recognized that (9) also contains the transformation used by Mangler (1948) for rotationally symmetrical boundary layers. From (8), (9) and (10) we obtain

$$u = u_e \frac{\partial f}{\partial \eta}, \tag{11a}$$

$$v = -\frac{r}{L} \frac{u_e}{(2\xi R)^{\frac{1}{2}}} \left\{ f + 2\xi \frac{\partial f}{\partial \xi} + (\Lambda - 1) \eta \frac{\partial f}{\partial \eta} \right\}. \tag{11b}$$

Here Λ is the ‘wedge variable’ defined by

$$\Lambda = \frac{2\xi du_e}{u_e d\xi} = 2\left(\frac{L V}{r u_e}\right)^2 \left\{ \int_0^x \frac{r^2 u_e dx}{L^2 V L} \right\} \frac{du_e/V}{dx/L}. \tag{12}$$

We remark that for pure wedge flow, $r = L$ and $u_e = cx^m$. It then follows from (12) that $\Lambda = 2m/(m + 1) = \text{const.}$ From (9) and (11) we derive

$$u \frac{\partial}{\partial x} + v \frac{\partial}{\partial y} = \frac{r^2 u_e^2}{2L^3 \xi V} \left\{ 2\xi \left(\frac{\partial f}{\partial \eta} \frac{\partial}{\partial \xi} - \frac{\partial f}{\partial \xi} \frac{\partial}{\partial \eta} \right) - f \frac{\partial}{\partial \eta} \right\}. \tag{13}$$

Making use of (4), (9), (11a), (12) and (13), the transformation of (1) is now easily obtained:

$$f''' + ff'' + \Lambda(1 - f'^2) = 2\xi \frac{\partial(f', f)}{\partial(\xi, \eta)}, \tag{14}$$

while the boundary conditions (5) become

$$\left. \begin{aligned} f + 2\xi \frac{\partial f}{\partial \xi} = 0, \quad \text{and} \quad f' = 0 \quad \text{for} \quad \eta = 0, \\ f' = 1 \quad \text{for} \quad \eta \rightarrow \infty. \end{aligned} \right\} \tag{15}$$

In (14) and (15) the accents refer to differentiation with respect to η , while on the right-hand side of (14) the Jacobian has been introduced as a convenient notation.

In order to transform (6), we introduce

$$T(x, y) = T_w + (T_e - T_w) \vartheta(\xi, \eta). \tag{16}$$

On the assumption that T_w and T_e do not depend on x , the thermal energy equation and its boundary conditions become

$$\vartheta'' + \sigma f \vartheta' = 2\xi \sigma \frac{\partial(\vartheta, f)}{\partial(\xi, \eta)}, \tag{17}$$

with $\vartheta = 0$ for $\eta = 0$, and $\vartheta = 1$ for $\eta \rightarrow \infty$. (18)

Herewith the transformations are completed, and we have now to solve the equations (14) and (17) with the boundary conditions (15) and (18) respectively. For that purpose we remark that in the boundary layer r depends only on x ; moreover, the dependence of u_e on x can be calculated from the potential theory or derived from experiments. Hence, ξ depends only on x , and for a given body we may consider x and u_e as known functions of ξ . As a result Λ is a known function of ξ . Inverting this function we may also say that for a given body, ξ is a function of Λ . The solution of (14) may thus be written as follows:

$$f(\xi, \eta) = f_0(\Lambda, \eta) + 2\xi \frac{d\Lambda}{d\xi} f_1(\Lambda, \eta) + \dots \tag{19}$$

Substituting (19) in (14) and (15), we get

$$\left. \begin{aligned} f_0''' + f_0 f_0'' + \Lambda(1 - f_0'^2) = 0, \\ f_0 = f_0' = 0 \quad \text{for} \quad \eta = 0, \quad \text{and} \quad f_0' = 1 \quad \text{for} \quad \eta \rightarrow \infty, \end{aligned} \right\} \tag{20}$$

$$\left. \begin{aligned} f_1''' + f_0 f_1'' - 2\Lambda f_0' f_1' + f_0'' f_1 = \frac{\partial(f_0', f_0)}{\partial(\Lambda, \eta)}, \\ f_1 = -\frac{\partial f_0}{\partial \Lambda}, \quad f_1 = 0 \quad \text{for} \quad \eta = 0, \quad \text{and} \quad f_1' = 0 \quad \text{for} \quad \eta \rightarrow \infty, \end{aligned} \right\} \tag{21}$$

and so on. The local friction coefficient is calculated from

$$c_f = \frac{\mu(\partial u/\partial y)_{y=0}}{\frac{1}{2}\rho V^2},$$

or, after transformation,

$$c_f R^{\frac{1}{2}} = 2 \frac{r}{L} \frac{(u_e/V)^2}{(2\xi)^{\frac{1}{2}}} \left(A_0 + 2\xi \frac{d\Lambda}{d\xi} A_1 + \dots \right), \tag{22}$$

where

$$A_k \equiv A_k(\Lambda) = f_k''(\Lambda, 0) \quad (k = 0, 1, 2, \dots). \tag{23}$$

In order to solve (17), we put

$$\vartheta(\xi, \eta) = \vartheta_0(\Lambda, \eta) + 2\xi \frac{d\Lambda}{d\xi} \vartheta_1(\Lambda, \eta) + \dots \tag{24}$$

Substituting (24) in (17) and (18), we then obtain

$$\left. \begin{aligned} \vartheta_0'' + \sigma f_0 \vartheta_0' &= 0, \\ \vartheta_0 &= 0 \text{ for } \eta = 0, \text{ and } \vartheta_0 = 1 \text{ for } \eta \rightarrow \infty, \end{aligned} \right\} \tag{25}$$

$$\left. \begin{aligned} \vartheta_1'' + \sigma f_0 \vartheta_1' &= -\sigma f_1 \vartheta_0' + \frac{\partial(\vartheta_0, f_0)}{\partial(\Lambda, \eta)}, \\ \vartheta_1 &= 0 \text{ for } \eta = 0, \text{ and } \vartheta_1 = 0 \text{ for } \eta \rightarrow \infty, \end{aligned} \right\} \tag{26}$$

and so on. The local Nusselt number is defined by

$$N = -\frac{(\partial T/\partial y)_{y=0}}{L(T_w - T_e)} = \frac{1}{L} \left(\frac{\partial \vartheta}{\partial y} \right)_{y=0},$$

or, after transformation,

$$\frac{N}{R^{\frac{1}{2}}} = \frac{r}{L} \frac{u_e/V}{(2\xi)^{\frac{1}{2}}} \left(E_0 + 2\xi \frac{d\Lambda}{d\xi} E_1 + \dots \right), \tag{27}$$

where

$$E_k \equiv E_k(\Lambda) = \vartheta_k'(\Lambda, 0) \quad (k = 0, 1, 2, \dots). \tag{28}$$

The transformations (9) and (10), and the expansions (19) and (24), are closely related to those being proposed by Görtler (1957). The latter author, however, expands the wedge variable Λ in terms of ξ . If this is done, Meksyn's original approximation method cannot be applied, so that Λ is retained here as an independent variable replacing the variable ξ . This is the principal difference between Meksyn's and Görtler's methods. According to Görtler, Meksyn's treatment involves the calculation of the potential flow around the body considered before attacking the boundary-layer problem. However, it is easily shown that the transformations (9) and (10) may be derived from those given by Meksyn if the equipotentials and streamlines around the given body are expressed in terms of the velocity of the potential flow around that body. We are therefore of the opinion that Meksyn's method is of great value for rapid boundary-layer calculations for any given $u_e(x)$.

The calculation of the local friction coefficient and the local Nusselt number may now proceed as follows. For a given body, r and u_e are known functions of x , so that for each value of x the quantities ξ , Λ , $d\Lambda/d\xi$, etc., can be calculated. Hence, for each value of x , the corresponding values of A_k and E_k can be determined from tables or diagrams representing A_k and E_k as functions of Λ and σ .

Thereupon, the local friction coefficient and the local Nusselt number are rapidly calculated from (22) and (27) respectively. As soon as A_k and E_k are known, this calculation can proceed very rapidly. A_0 has been calculated by Hartree (1937), while E_0 has been calculated by Eckert (1942) for $\sigma = 0.7, 0.8, 1, 5$ and 10 . As far as we know, A_k and E_k for $k \geq 1$ have not been calculated as yet. However, for the application of a pure wedge method we need only A_0 and E_0 , since for wedge-shaped profiles (for which $\Lambda = \text{constant}$) only the first terms at the right-hand sides of (19), (22), (24) and (27) are retained, while all other terms vanish. As a result, application of a pure wedge method to arbitrary two-dimensional profiles or rotationally symmetrical bodies means that only the first terms at the right-hand sides of (22) and (27) have to be retained (this approximation will be called Meksyn's wedge method). Since A_1 and E_1 are finite, this procedure is legitimate if ξ and/or $d\Lambda/d\xi$ are small. Generally speaking, this is the case in the vicinity of the forward stagnation point. At some distance from the forward stagnation point the second terms in (22) and (27) also become important. However, comparing the results obtained by Meksyn's wedge method with those obtained by the wedge methods mentioned in § 1, it appears that the accuracy of Meksyn's wedge method is of the same order of magnitude as that of the others. This demonstrates the rapid convergence of the series (22) and (27). It may be expected that even in the vicinity of the separation point of the boundary layer the series (22) and (27) yield satisfactory results if only two terms are retained.

Finally, we remark that the same method may be used if the assumptions IV and V are rejected. For gases it is, for example, convenient to apply first Stewartson's (1950) transformation (see also Cohen & Reshotko 1955) to the boundary-layer equations, whereupon 'wedge coordinates' analogous to those defined by (9) may be introduced. It is also possible to account for variations in the temperature of the wall. We have made analogous calculations for unsteady two-dimensional boundary layers. For unsteady rotationally symmetrical boundary layers the method fails, because then it is no longer possible to apply Mangler's transformation.

Using Meksyn's wedge method, we have also performed mass transfer calculations accounting for a velocity normal to the wall of the body. All these modifications of Meksyn's wedge method are not treated in this paper, because we intend to discuss only the principles of this method and not all its possible extensions.

3. Asymptotic expansion of the Nusselt number for a flat plate

We shall now discuss how the Nusselt number may be represented explicitly as a function of the Prandtl number. For that purpose we consider first the most simple case, viz. that of the flat plate without a longitudinal pressure gradient. In that case we have $r = L$, $u_e = V$, $\Lambda = 0$, $f = f_0$ and $\vartheta = \vartheta_0$. Hence, (27) becomes

$$\frac{N}{R^{\frac{1}{2}}} = \left(\frac{L}{2x}\right)^{\frac{1}{2}} E.$$

Averaging the Nusselt number over the length L of the plate, we get

$$\frac{\bar{N}}{R^{\frac{1}{2}}} = \frac{1}{L} \int_0^L \frac{N}{R^{\frac{1}{2}}} dx = 2^{\frac{1}{2}} E. \quad (29)$$

In the same manner the average value of the friction coefficient is obtained from (22), yielding

$$\bar{c}_f R^{\frac{1}{2}} = 2^{\frac{1}{2}} A. \tag{30}$$

In order to calculate E , we derive from (25), for $\vartheta = \vartheta_0$ and $f = f_0$,

$$\frac{1}{E} = \int_0^\infty \exp(-\sigma F) d\eta, \tag{31}$$

where

$$F \equiv F(\eta) = \int_0^\eta f(\eta) d\eta. \tag{32}$$

Formula (31) has been worked out by several authors. First of all we mention the exact calculations performed by E. Pohlhausen (1921). Other authors remarked that for large values of the Prandtl number the thickness δ_T is only a small fraction of the thickness δ , so that for the calculation of E the velocity profile in the thermal boundary layer may be linearized, that is, in (31) the function F may be represented by $\frac{1}{2} A \eta^2$. This procedure has already been applied by Falkner & Skan (1930, 1931), while the approximate calculations made by Piercy & Preston (1936) are in fact based upon the same principle. Lighthill (1950) developed an elegant method of calculating the heat transfer in laminar boundary layers, which is also based upon linearized velocity profiles. Tifford (1951), remarking that Lighthill's results are only valid for high values of the Prandtl number, modified Lighthill's formulae in order to obtain results valid for $\sigma \doteq 1$.

Frössling (1940) and Schuh (1949, 1954) also discussed the limit $\sigma \rightarrow \infty$, while Davies & Bourne (1956) developed a method where the velocity profile is represented by $c\eta^n$, n being determined in such a way that the results for $\sigma \doteq 1$ agree as closely as possible with the exact solution. Finally we may mention a paper by Morgan & Warner (1956) containing a survey of applications of heat transfer calculations in the limit $\sigma \rightarrow \infty$.

In the papers mentioned above, the formulae for the Nusselt number represent the first term of an asymptotic expansion for high values of the Prandtl number. In order to obtain formulae for lower values of σ , the expansion has to be extended. This may be done in several ways. An obvious way is to substitute $\tau = F$ in (31) and to consider τ as a new integration variable. In that way (31) becomes

$$\frac{1}{E(\sigma)} = \int_0^\infty e^{-\sigma\tau} \frac{d\eta}{d\tau} d\tau. \tag{33}$$

This formula shows that $1/E(\sigma)$ may be considered as the Laplace transform of $d\eta/d\tau$. Hence, the asymptotic expansion of $1/E(\sigma)$ may be obtained by means of Abel's well-known asymptotic theorem (see, for instance, Doetsch 1943). In order to apply this theorem we have to expand $F(\eta)$ in a power series. Putting $\Lambda = 0$, the expansion of $f = f_0$ is easily derived from (20). This expression has already been derived by Blasius (1908) and reads on as follows:

$$\tau \equiv F = A \frac{\eta^3}{3!} - A^2 \frac{\eta^6}{6!} + 11A^3 \frac{\eta^9}{9!} - 375A^4 \frac{\eta^{12}}{12!} + O(\eta^{15}), \tag{34}$$

where O is the well-known Bachmann-Landau symbol. Inversion of (34) yields

$$\eta = \left(\frac{6\tau}{A}\right)^{\frac{1}{3}} \left\{ 1 + \frac{1}{60}\tau - \frac{1}{1,260}\tau^2 + \frac{23}{891,000}\tau^3 + O(\tau^4) \right\}. \tag{35}$$

Substituting (35) in (33), we obtain

$$\frac{1}{E(\sigma)} = \frac{1}{3} \left(\frac{6}{A}\right)^{\frac{1}{2}} \int_0^\infty e^{-\sigma\tau} \tau^{-\frac{3}{2}} \left\{ 1 + \frac{1}{15}\tau - \frac{1}{180}\tau^2 + \frac{23}{89,100}\tau^3 + O(\tau^4) \right\} d\tau.$$

On term-by-term integration of the right-hand side of the last equation, an asymptotic expansion is obtained. Since the reciprocal of an asymptotic expansion is again an asymptotic expansion, a simple calculation brings forth the following result:

$$E(\sigma) = \frac{(A\sigma/6)^{\frac{1}{2}}}{\Gamma(\frac{4}{3})} \left\{ 1 - \frac{1}{45}\sigma^{-1} + \frac{2}{675}\sigma^{-2} - \frac{1,168}{3,007,125}\sigma^{-3} + O(\sigma^{-4}) \right\}, \quad (36)$$

$\bar{N}/R^{\frac{1}{2}}$						
Asymptotic expansion (37)						
σ	1 term	2 terms	3 terms	4 terms	Exact	Tifford
0.1	—	—	—	0.2846	0.2762	0.294
0.5	0.5377	0.5138	0.5202	0.5185	0.5182	0.520
0.6	0.5714	0.5502	0.5549	0.5539	0.5537	0.554
0.7	0.6015	0.5824	0.5860	0.5853	0.5853	0.585
0.8	0.6289	0.6114	0.6143	0.6138	0.6138	0.614
0.9	0.6541	0.6380	0.6403	0.6400	0.6400	0.640
1.0	0.6775	0.6624	0.6644	0.6641	0.6641	0.664
1.1	0.6994	0.6853	0.6870	0.6868	0.6868	0.687
7	1.2959	1.2918	1.2919	1.2919	1.2919	1.32
10	1.4595	1.4563	1.4563	1.4563	1.4563	1.50
15	1.6708	1.6683	1.6683	1.6683	1.6682	1.73

TABLE I

where Γ denotes the gamma-function. The coefficient A has been calculated by Blasius (1908) and by Töpfer (1912). According to the latter author we have $A = 0.33206\sqrt{2} = 0.46960$, while $\Gamma(\frac{4}{3}) = 0.89298$. Substituting (36) in (29) and making use of the given values of A and $\Gamma(\frac{4}{3})$, we obtain

$$\frac{\bar{N}}{R^{\frac{1}{2}}} = 0.6775\sigma^{\frac{1}{2}} \left\{ 1 - \frac{1}{45}\sigma^{-1} + \frac{2}{675}\sigma^{-2} - \frac{1,168}{3,007,125}\sigma^{-3} + O(\sigma^{-4}) \right\}. \quad (37)$$

The Nusselt number calculated by means of (37) may be compared with the exact calculations made by E. Pohlhausen (1921). For that purpose we have extended Pohlhausen's calculations in order to obtain results in four figures (Pohlhausen gives only three figures), while we have also performed calculations for $\sigma = 0.5$ and 0.1 . The results are shown in table 1, where values calculated by means of Tifford's (1951) formula are also included. For a flat plate Tifford's formula reads

$$\frac{\bar{N}}{R^{\frac{1}{2}}} = 0.664\sigma^{0.35}. \quad (38)$$

Table 1 shows that Tifford's formula yields satisfactory results if $\sigma \doteq 1$; for very high and low values of the Prandtl number formula (38) fails. Furthermore,

it appears that for $\sigma \geq 0.5$ our expansion (37) leads to surprisingly good results even to the fourth decimal place. Even for $\sigma = 0.1$, this expansion may be used if its convergence is improved by means of Euler's transformation (for $\sigma \geq 0.5$, Euler's transformation does not improve the convergence), since the value calculated by (37) is then only about 3% too high.

Table 1 indicates how many terms of the expansion have to be retained. For $\sigma \geq 1$, two terms of the expansion are sufficient if the desired accuracy is not higher than 0.3%. For $\sigma \geq 10$, one term is sufficient.

For $\sigma = 1$, we have $\vartheta = f'$, so that apparently the expansion (37) may also be used to calculate A . This has already been proposed by Meksyn (1950, 1955, 1956), who worked out this method to calculate the friction coefficients and separation points of boundary layers with longitudinal pressure gradient. As far as we know this author did not derive expansions of type (37) showing the dependence of the Nusselt number on the Prandtl number.

4. Asymptotic expansion of E_0 for arbitrary values of the wedge variable

We shall now show that by the asymptotic method one can also easily calculate the transfer coefficients for $\Lambda \neq 0$, i.e. for boundary layers with longitudinal pressure gradient. For that purpose we calculate E_0 from (25). Again we have

$$\frac{1}{E_0} = \int_0^\infty \exp(-\sigma F_0) d\eta, \tag{39}$$

F_0 being given by

$$F_0(\eta) = \int_0^\eta f_0(\eta) d\eta. \tag{40}$$

From (20) we derive

$$f_0 = A_0 \frac{\eta^2}{2!} - \Lambda \frac{\eta^3}{3!} + A_0^2(2\Lambda - 1) \frac{\eta^5}{5!} + O(\eta^6),$$

where A_0 is defined by (23). From the last expansion we obtain

$$\tau \equiv F_0 = A_0 \frac{\eta^3}{3!} - \Lambda \frac{\eta^4}{4!} + A_0^2(2\Lambda - 1) \frac{\eta^6}{6!} + O(\eta^7),$$

or, after inversion,

$$\eta = \left(\frac{6}{A_0}\right)^{\frac{1}{3}} \tau^{\frac{1}{3}} \left\{ 1 + \frac{\Lambda}{72} \left(\frac{6}{A_0}\right)^{\frac{1}{3}} \tau^{\frac{1}{3}} + \frac{\Lambda^2}{1728} \left(\frac{6}{A_0}\right)^{\frac{2}{3}} \tau^{\frac{2}{3}} + \left(\frac{35}{864} \frac{\Lambda^3}{A_0^4} - \frac{2\Lambda - 1}{60}\right) \tau + O(\tau^{\frac{4}{3}}) \right\}. \tag{41}$$

Substituting (41) in (39), we may use the same method as in § 3. The result of the calculations is given by

$$\begin{aligned} \frac{1}{E_0} = \frac{1}{3} \Gamma\left(\frac{1}{3}\right) \left(\frac{6}{A_0 \sigma}\right)^{\frac{1}{3}} & \left\{ 1 + \frac{\Lambda}{36} \frac{\Gamma\left(\frac{2}{3}\right)}{\Gamma\left(\frac{1}{3}\right)} \left(\frac{6}{A_0}\right)^{\frac{1}{3}} \sigma^{-\frac{1}{3}} + \frac{\Lambda^2}{576} \frac{\Gamma(1)}{\Gamma\left(\frac{1}{3}\right)} \left(\frac{6}{A_0}\right)^{\frac{2}{3}} \sigma^{-\frac{2}{3}} \right. \\ & \left. + \frac{1}{3} \left(\frac{35}{216} \frac{\Lambda^3}{A_0^4} - \frac{2\Lambda - 1}{15}\right) \sigma^{-1} + O(\sigma^{-\frac{4}{3}}) \right\}. \end{aligned}$$

From this expansion it follows (with $\Gamma(\frac{1}{3}) = 2.6789$ and $\Gamma(\frac{2}{3}) = 1.3541$) that

$$E_0 = 0.6163(A_0\sigma)^{\frac{1}{3}} \left\{ 1 - 0.1531\Lambda A_0^{-\frac{1}{3}}\sigma^{-\frac{1}{3}} - 0.0536\Lambda^2 A_0^{-\frac{2}{3}}\sigma^{-\frac{2}{3}} + \left(\frac{2\Lambda - 1}{45} - 0.03402\Lambda^3 A_0^{-4} \right) \sigma^{-1} + O(\sigma^{-\frac{4}{3}}) \right\}. \quad (42)$$

The quantity A_0 has been calculated by Hartree (1937) and in figure 1 is represented as a function of Λ for $-0.1988 \leq \Lambda \leq 1$. In order to show that the

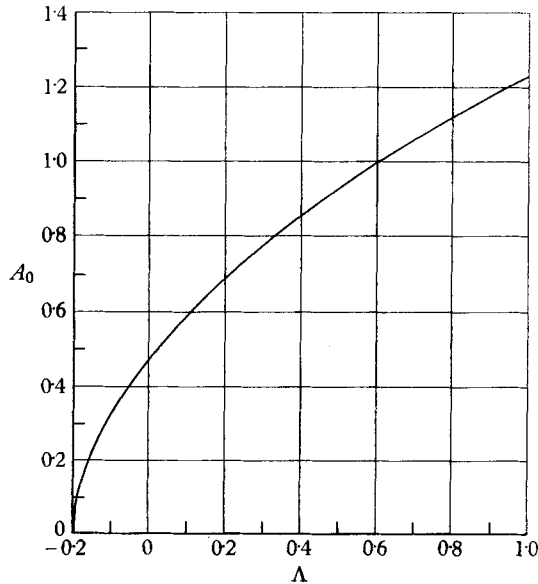


FIGURE 1. A_0 as a function of the wedge variable Λ , according to Hartree (1937).

Λ	E_0 for $\sigma = 1$	
	Eckert	Expansion (42)
1.0	0.5704	0.5689 (-0.3%)
0.5	0.5390	0.5370 (-0.4%)
0.0	0.4696	0.4684 (-0.3%)
-0.14	0.4160	0.4196 (+0.9%)

TABLE 2

expansion (42) may be used for finite values of the Prandtl numbers, we compare the values calculated from (42) with those calculated exactly by Eckert (1942). Table 2 shows that expansion (42) leads to satisfactory results for $\sigma = 1$. For $\sigma \geq 0.7$, the expansion is even more accurate than the interpolation formula proposed by Eckert (1942). Furthermore, table 2 shows that the accuracy of the expansion decreases as Λ decreases. This is due to the fact that A_0 approaches zero if Λ approaches -0.1988 . For $A_0 = 0$, the expansion (42) is meaningless and

has to be replaced by another expansion. Putting $A_0 = 0$ ($\Lambda = -0.1988$), we derive from (20)

$$f_0 = -\Lambda \frac{\eta^3}{3!} - 2\Lambda^2(2-3\Lambda) \frac{\eta^7}{7!} - 16\Lambda^3(2-3\Lambda)(8-7\Lambda) \frac{\eta^{11}}{11!} + O(\eta^{15}).$$

Applying the same technique as before, we find

$$\eta = \left(\frac{24}{-\Lambda}\right)^{\frac{1}{2}} \tau^{\frac{1}{2}} \left[1 + \frac{1}{140} (2-3\Lambda)\tau + \left\{ \frac{13}{39,200} (2-3\Lambda)^2 - \frac{2(2-3\Lambda)(8-7\Lambda)}{17,325} \right\} \tau^2 + O(\tau^3) \right]. \quad (43)$$

Substituting (43) in (39) and putting $\Lambda = -0.1988$, we obtain

$$E_0 = 0.3328\sigma^{\frac{1}{2}} \{ 1 - 0.02318\sigma^{-1} + 0.00001345\sigma^{-2} + O(\sigma^{-3}) \}. \quad (44)$$

For $\sigma = 0.7$ this expansion yields $E_0 = 0.2943$, while according to the exact calculations made by Brown & Donoughe (1951) we should have $E_0 = 0.2939$. Since in both cases the fourth figure is not reliable, the agreement is satisfactory.

Λ	...	1.6	1.0	0.5	0.2	0	-0.14	-0.1988
η^*		0.5439	0.6479	0.8044	0.9839	1.2167	1.5967	2.3587

TABLE 3

It is also possible to derive expansions valid for very low values of the Prandtl number. In this case the thickness of the dynamic boundary layer is only a small fraction of the thickness of the thermal boundary layer. This means that in (39) f_0 may now be approximated by the asymptotic expansion in terms of η . Since $f'_0 = 1$ for $\eta \rightarrow \infty$, we may write

$$f_0 \sim \eta - \eta^*, \quad (45)$$

where η^* may be interpreted as a reduced displacement thickness defined by

$$\eta^* = \lim_{\eta \rightarrow \infty} \int_0^\eta (1 - f'_0) d\eta = \lim_{\eta \rightarrow \infty} \{ \eta - f_0(\eta) \}.$$

Substituting (45) in (39), we obtain

$$E_0 = (2\sigma/\pi)^{\frac{1}{2}} \frac{\exp(-\frac{1}{2}\eta^{*2}\sigma)}{1 + \operatorname{erf}\{\eta^*(\frac{1}{2}\sigma)^{\frac{1}{2}}\}}, \quad (46)$$

where $\operatorname{erf}(z) = \frac{2}{\sqrt{\pi}} \int_0^z e^{-y^2} dy$.

For low values of the Prandtl number, the right-hand side of (46) may be expanded further. The result is

$$E_0 = (2\sigma/\pi)^{\frac{1}{2}} [1 - \eta^*(2\sigma/\pi)^{\frac{1}{2}} + \dots]. \quad (47)$$

Values for η^* have been provided by Eckert (1942), and are given in table 3.

The interpretation of (47) is obvious: the first term at the right-hand side of (47) represents the heat transfer in a potential flow and agrees with the formulae derived by Boussinesq (1903, 1905). This interpretation is in accordance with the considerations in §1. The second term in (47) represents a first-order correction accounting for small viscosity effects. For flat plates, formula (47) has been discussed by Sparrow & Gregg (1957). These authors show that (at least for flat plates) (47) yields satisfactory results for values of the Prandtl number smaller than about 0.03.

Finally, in figure 2, E_0 is represented as a function of Λ for some values of the Prandtl number.

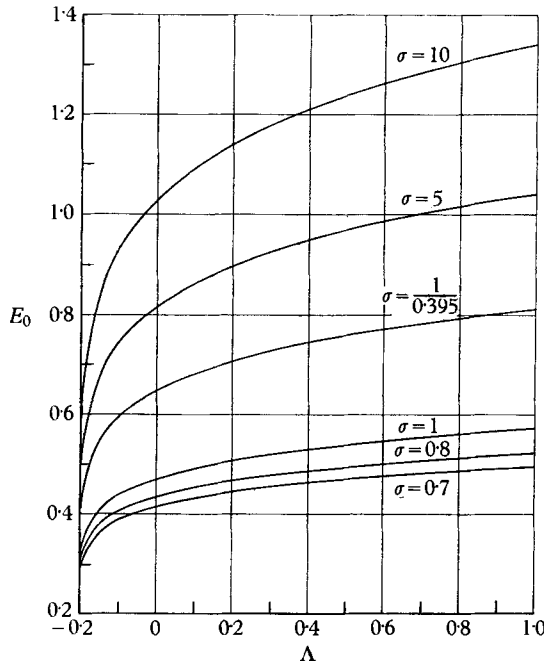


FIGURE 2. E_0 as a function of the wedge variable Λ , for some values of the Prandtl number.

5. Application to the calculation of the local heat transfer

Meksyn (1947, 1948) has already given some applications to the calculation of the local friction coefficient, so that we shall confine ourselves to the calculation of the local heat transfer. Let us first consider some two-dimensional profiles, viz. elliptical cylinders. The elliptical profile is determined by the ratio a/b of its semi-axes, a being parallel to the oncoming flow (see figure 3). The case $a/b = 1$ represents the circular cylinder, and $a/b = \infty$ the flat plate parallel to the direction of the oncoming flow. Furthermore, we shall consider the cases $a/b = 2$ and 4. The reference length L will be defined by $L = 2a$.

In order to calculate the wedge variable we have to know u_e as a function of x . For elliptical cylinders the potential theory yields

$$\left(\frac{u_e}{V}\right)^2 = \left(1 + \frac{a}{b}\right)^2 \frac{1 - \cos 2\phi}{1 + (a/b)^2 + \{1 - (a/b)^2\} \cos 2\phi}, \quad (48)$$

where ϕ is the angular coordinate (see figure 3). Since we have taken for our two-dimensional profiles $r = L$, we obtain from (12) and (48)

$$\Lambda = \frac{4}{1 + (a/b)^2 + \{1 - (a/b)^2\} \cos 2\phi} \frac{\cos \phi}{1 + \cos \phi} \tag{49}$$

Formula (48) is the more reliable the more slender the elliptical profiles. For broad profiles the wake behind the cylinder has an important influence on u_e , and

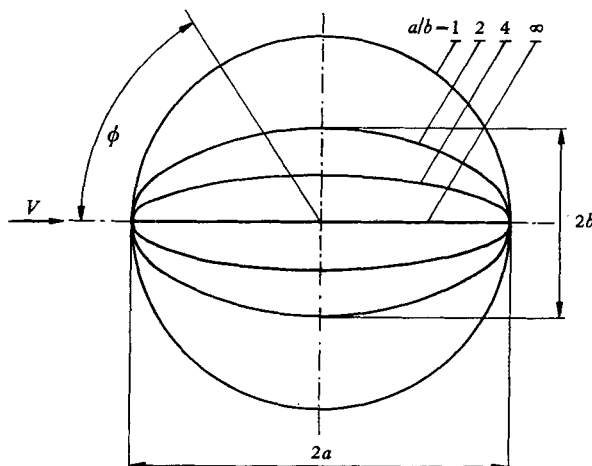


FIGURE 3. Sketch of the elliptical profiles considered in the text.

this influence is not accounted for in (48). Hence, for circular cylinders it is advisable to derive u_e from experiments instead of from (48). For that purpose u_e is written as

$$u_e/V = u_1(x/L) - u_3(x/L)^3 - u_5(x/L)^5,$$

where L is now equal to the diameter of the cylinder. According to Hiemenz (1911) we have

$$u_1 = 3.631, \quad u_3 = 2.171, \quad u_5 = 1.514$$

for $R = 18,500$, while according to the measurements made by Schmidt & Wenner (1941) we have

$$u_1 = 3.631, \quad u_3 = 3.275, \quad u_5 = 0.168$$

for $R = 170,000$.

In figure 4 the curves of the wedge variable are given. For $a/b = 1$, three curves are given, which are all calculated from (12) for $r = L$. The calculation of the solid curve is based upon u_e according to the potential theory, that of the dashed curve upon u_e according to the measurements made by Schmidt & Wenner (1941), and that of the dash-dotted curve upon u_e according to the measurements made by Hiemenz (1911).

Figure 4 shows that in the vicinity of the forward stagnation point $d\Lambda/dx \doteq 0$, while moreover ξ is small. Hence, in this region Meksyn's wedge method is near to the mark. If a/b increases, this region decreases, but at the same time the slope of the (Λ, x) -curves at median values of x/L becomes smaller, indicating that at median values of x/L Meksyn's wedge method is fairly accurate. This is to be

expected, since slender profiles behave approximately like flat plates and for these Meksyn's wedge method is exact.

At the vicinity of the separation point of the boundary layer, which according to Hartree (1937) is determined by $\Lambda = -0.1988$, the slope of the (Λ, x) -curves is large, so that in this region the method is no longer reliable. This may also be demonstrated by means of the calculated position of the separation point. Denoting the separation point by suffix s , we obtain from the wedge method $\phi_s = 95.2^\circ$ for a circular cylinder (u_e according to the potential theory), while the series expansion of Blasius leads to $\phi_s = 110^\circ$. If u_e is represented by the measurements made by Schmidt & Wenner, we then find $\phi_s = 72.4^\circ$, while the experimental value is given by $\phi_s \doteq 80^\circ$. For the elliptical cylinder with $a/b = 2$ and u_e

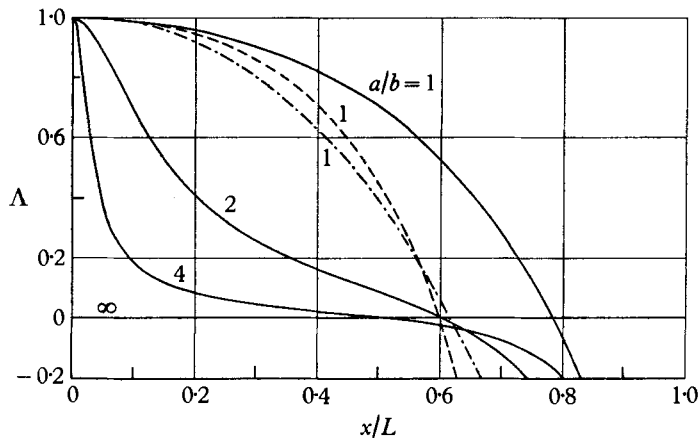


FIGURE 4. Wedge variable for elliptical profiles; solid curves according to the potential theory, dashed curve according to Schmidt & Wenner (1941), dash-dotted curve according to Hiemenz (1911).

according to the potential theory, we get from Meksyn's wedge method $\phi_s = 105.8^\circ$, from Eckert's wedge method $\phi_s = 115^\circ$, and from the integral method of Pohlhausen $\phi_s = 120.8^\circ$. Apparently the separation points calculated from Meksyn's zero-order approximation are too low.

In figure 5 the local Nusselt numbers are given for the circular cylinder for $\sigma = 0.7, 1, 5$ and 10 . The calculations are based upon the velocity distribution measured by Schmidt & Wenner. For $\sigma = 0.7$ the calculations may be compared with those of Eckert (1942) and Frössling (1940). In figure 5 the dashed curve is calculated by Eckert and the dash-dotted curve by Frössling. For $\phi < 50^\circ$ the agreement is satisfactory, but for higher values of ϕ discrepancies exist. Frössling's calculations are based upon series expansions in terms of x/L containing only three terms, so that Frössling's curve is no longer reliable for $\phi > 50^\circ$. Hence, it is not possible to decide whether Eckert's or our curve is to be preferred. In figure 6 the local Nusselt numbers calculated from Meksyn's wedge method are compared with those measured by Schmidt & Wenner. The three calculated curves correspond to those given in figure 4 for $a/b = 1$. The curve calculated by means of the velocity distribution measured by Schmidt & Wenner is satisfactory, though the theoretical value at the forward stagnation point is too low (it has to be borne in

mind that at this point the theoretical value is exact). The curve calculated by Eckert (not given in figure 6) gives a worse fit to the experimental curves, since Eckert's curve is too flat in the vicinity of the separation point. As far as we know, no calculations have as yet been performed for values of σ other than 0.7, so that we cannot compare our calculations with others for $\sigma = 1, 5$ and 10.

In figure 7 the local Nusselt number is given for the elliptical profile with $a/b = 2$. The dashed curve is calculated by Eckert. At the separation point this curve is again higher than ours.

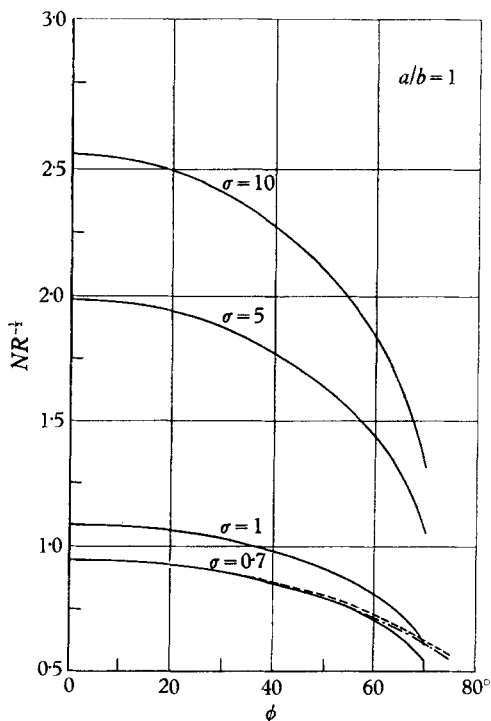


FIGURE 5. The local Nusselt number for circular cylinders; solid curves are calculated according to Meksyn's method, dashed curve according to Eckert (1942), dash-dotted curve according to Frössling (1940).

In figure 8 the calculations are represented for elliptical profiles with $a/b = 4$. In this case the difference between Eckert's calculations and ours is negligible.

For $\sigma > 10$ the calculations may be performed by means of the first term of the expansion (42), so that

$$E_0(\Lambda, \sigma) = 0.6163\{A_0(\Lambda) \sigma\}^{\frac{1}{2}}. \tag{50}$$

At the separation point we obtain from (44)

$$E_0(-0.1988, \sigma) = 0.3328\sigma^{\frac{1}{2}}. \tag{51}$$

Hence, if the quantity $N/(R^{\frac{1}{2}}\sigma^{\frac{1}{2}})$ is plotted against x , then in the limiting case $\sigma \rightarrow \infty$ the curves approach zero as x approaches the separation point, though the local heat transfer at this point is not zero. The results of the calculations are shown in figure 9. Together with figures 5, 7 and 8, figure 9 shows the behaviour of the local heat transfer of elliptical cylinders for $\sigma \geq 0.7$.

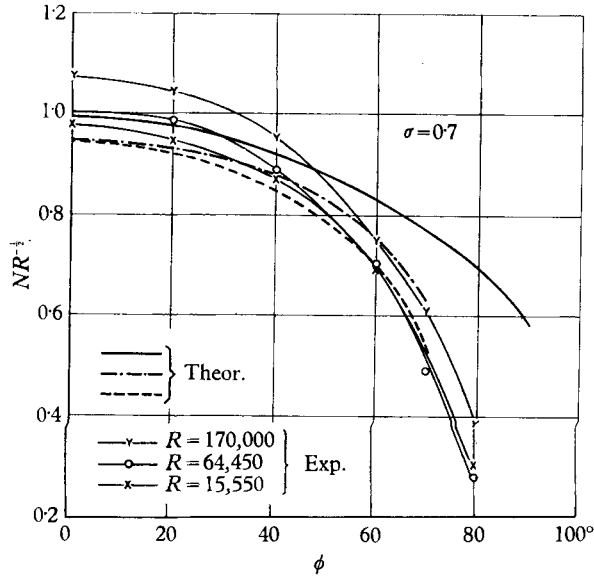


FIGURE 6. Comparison between calculated and measured local Nusselt numbers for circular cylinders at $\sigma = 0.7$.

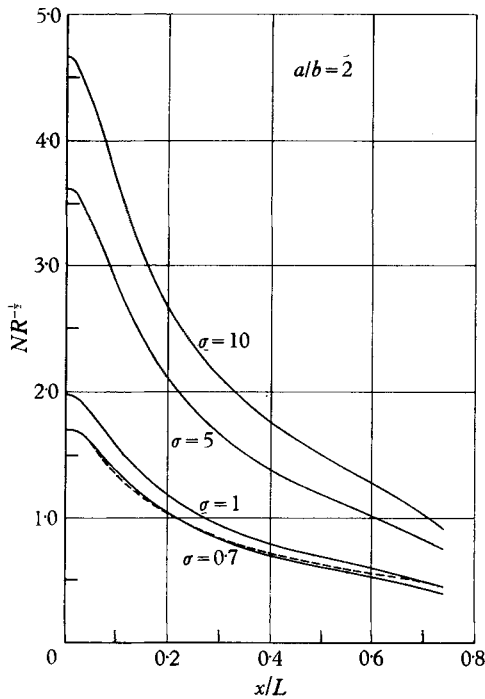


FIGURE 7. The local Nusselt number for an elliptical profile with $a/b = 2$; the dashed curve is calculated by Eckert (1942).

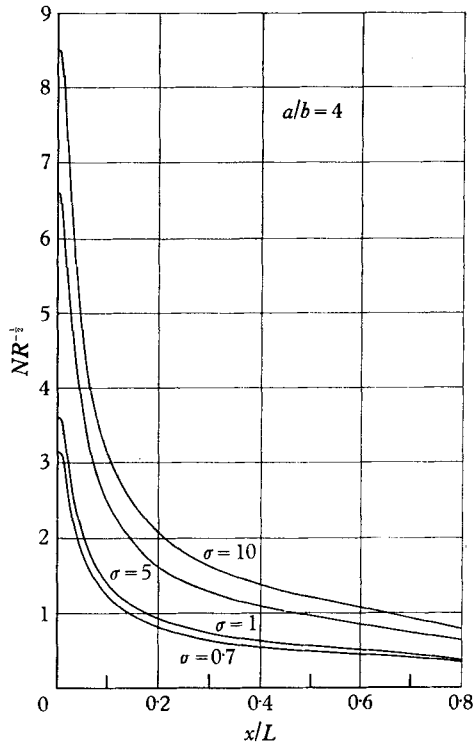


FIGURE 8. The local Nusselt number for an elliptical profile with $a/b=4$.

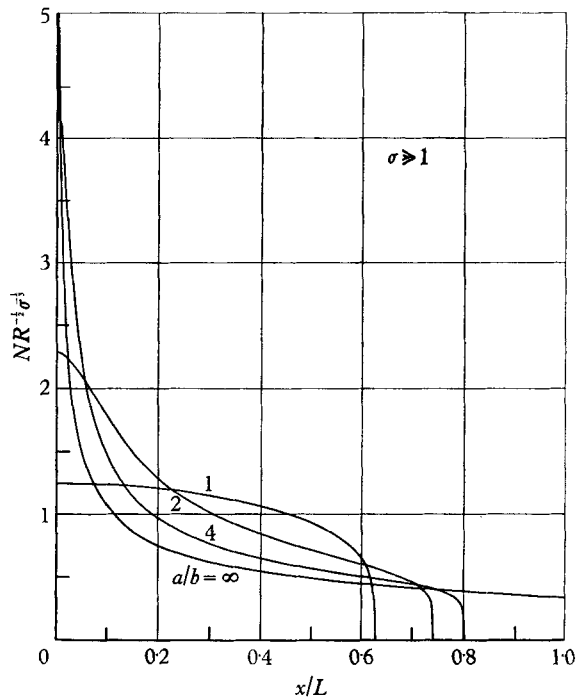


FIGURE 9. The local Nusselt number for some elliptical profiles at $\sigma \geq 1$.

Finally, we shall discuss the application to spheres. Putting L equal to the diameter of the sphere, we have

$$r/L = \frac{1}{2} \sin \phi = \frac{1}{2} \sin (2x/L). \quad (52)$$

The velocity u_e may be derived from the measurements made by Fage for $R = 157,200$. Frössling (1940) represented these measurements by

$$u_e/V = 3(x/L) - 3.4966(x/L)^3 + 4.7391(x/L)^5 - 5.1481(x/L)^7. \quad (53)$$

From (52) and (53) the wedge variable can be calculated, whereupon the local Nusselt number is easily computed by means of Meksyn's wedge method. The

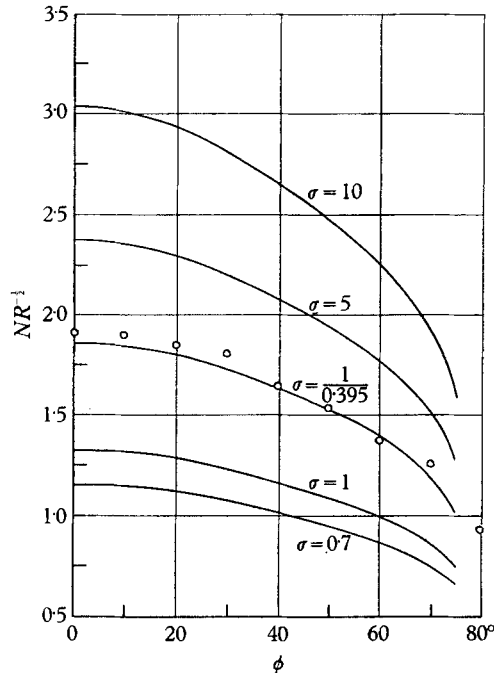


FIGURE 10. The local Nusselt number for spheres; the dots represent the measurements made by Frössling (1940) at $\sigma = 1/0.395$.

results are shown in figure 10. We have also performed the calculations for $\sigma = 1/0.395 = 2.56$. This curve may be compared with the measurements made by Frössling (1938). The agreement between experiment and theory is surprisingly good, but may be accidental, because the measurements were performed at $R = 1060$ while the calculations are based upon the velocity distribution of Fage measured at $R = 157,200$.

Figure 11 represents the local Nusselt number for $\sigma \gg 1$ (say $\sigma > 10$). Comparing this curve with the corresponding curve for the circular cylinder, it appears that under equal conditions the local heat flux of spheres is higher than that of circular cylinders. This may be explained physically by the spatial divergence of the streamlines in the boundary layer of the sphere, which is lacking in the boundary layer of the circular cylinder. Under equal conditions this effect makes the boundary layer of the sphere thinner than that of the circular cylinder.

This paper is a part of a doctoral thesis presented at the Technological University at Delft. The author is indebted to Prof. Dr J. A. Prins of the Technological University for helpful discussions and suggestions.

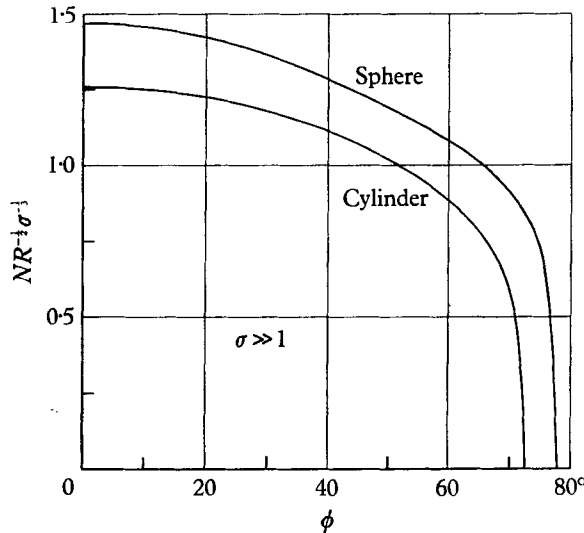


FIGURE 11. The local Nusselt number for spheres and circular cylinders at $\sigma \gg 1$.

REFERENCES

- BLASIUS, H. 1908 *Z. Math. Phys.* **56**, 1; also *Nat. Adv. Comm. Aero., Wash., Tech. Mem.* no. 1256.
- BOUSSINESQ, J. 1903 *Théorie Analytique de la Chaleur*, vol. II. Paris: Gauthier-Villars.
- BOUSSINESQ, J. 1905 *J. Math. Pures Appl.* **1**, 285.
- BROWN, W. B. & DONOUGHE, P. L. 1951 *Nat. Adv. Comm. Aero., Wash., Tech. Note*, no. 2479.
- COHEN, C. B. & RESHOTKO, E. 1955 *Nat. Adv. Comm. Aero., Wash., Tech. Note*, no. 3326.
- DAVIES, D. B. & BOURNE, D. E. 1956 *Quart. J. Mech. Appl. Math.* **9**, 457.
- DOETSCH, G. 1943 *Theorie und Anwendung der Laplace-Transformation*. New York: Dover.
- DREW, T. B. 1931 *Trans. Amer. Inst. Chem. Engrs*, **26**, 6.
- ECKERT, E. 1942 *V.D.I.-Forschungsheft* **416**.
- ECKERT, E. & LIVINGOOD, J. N. B. 1953 *Nat. Adv. Comm. Aero., Wash., Rep.* no. 1118.
- FALKNER, V. M. & SKAN, S. W. 1930 *Aero. Res. Coun. Lond., Rep. & Mem.* no. 1314; also *Phil. Mag.* (7), **12**, 865 (1931).
- FRÖSSLING, N. 1938 *Beitr. Geophys.* **52**, 170.
- FRÖSSLING, N. 1940 *Lunds Univ. Årsskr., N.F. Avd.* **2**, **36**, no. 4.
- GÖRTLER, H. 1939 *Z. angew. Math. Mech.* **19**, 129.
- GÖRTLER, H. 1957 *J. Math. Mech.* **6**, 1.
- HARTREE, D. R. 1937 *Proc. Camb. Phil. Soc.* **33**, 223.
- HIEMENZ, K. 1911 Dissertation, Göttingen; also *Dinglers Polytech. J.* **326**, 32 (1911).
- KÁRMÁN, TH. VON 1921 *Z. angew. Math. Mech.* **1**, 233; also *Nat. Adv. Comm. Aero., Wash., Tech. Mem.* no. 1092.
- KOTSCHIN, N. J., KIBEL, I. A. & ROSE, N. W. 1955 *Theoretische Hydromechanik II*, *Akad. Verlag, Berlin*, p. 399.
- LIGHTHILL, M. J. 1950 *Proc. Roy. Soc. A*, **202**, 359.
- MANGLER, W. 1948 *Z. angew. Math. Mech.* **28**, 97.

- MEKSYN, D. 1947 *Proc. Roy. Soc. A*, **192**, 545, 567.
MEKSYN, D. 1948 *Proc. Roy. Soc. A*, **194**, 218.
MEKSYN, D. 1950 *Proc. Roy. Soc. A*, **201**, 268, 279.
MEKSYN, D. 1955 *Proc. Roy. Soc. A*, **231**, 274.
MEKSYN, D. 1956 *Proc. Roy. Soc. A*, **237**, 543.
MORGAN, G. W. & WARNER, W. H. 1956 *J. Aero. Sci.* **23**, 937.
PIERCY, N. A. V. & PRESTON, J. H. 1936 *Phil. Mag.* **21**, 995.
POHLHAUSEN, E. 1921 *Z. angew. Math. Mech.* **1**, 115.
POHLHAUSEN, K. 1921 *Z. angew. Math. Mech.* **1**, 252.
PRANDTL, L. 1904 *Proc. 3rd Int. Math. Congr., Heidelberg*, p. 484.
PRANDTL, L. 1938 *Z. angew. Math. Mech.* **18**, 77; also *Nat. Adv. Comm. Aero., Wash., Tech. Mem.* no. 959.
SCHMIDT, E. & WENNER, K. 1941 *Forsch. Ing.-Wes.* **12**, 65.
SCHUH, H. 1949 *Temperaturgrenzsichten. Göttinger Monographien*, B, **6**.
SCHUH, H. 1954 *Forsch. Ing.-Wes.* **20**, 37.
SMITH, A. M. O. 1956 *J. Aero. Sci.* **23**, 901.
SPARROW, E. M. & GREGG, J. L. 1957 *J. Aero. Sci.* **24**, 852.
STEWARTSON, K. 1950 *Proc. Roy. Soc. A*, **200**, 84.
TIFFORD, A. N. 1951 *J. Aero. Sci.* **18**, 283.
TÖPFER, C. 1912 *Z. Math. Phys.* **60**, 397.